NIH-PA Author Manuscript

FRET-Labeled siRNA Probes for Tracking Assembly and Disassembly of siRNA-Nanocomplexes

Christopher A. Alabi[1,2], **Kevin T. Love**[1], **Gaurav Sahay**[1], **Tina Stutzman**[4], **Whitney T. Young**[5], **Robert Langer**[1,2,3], and **Daniel G. Anderson**[1,2,3,†]

[1]David H. Koch Institute for Integrative Cancer Research, Massachusetts Institute of Technology, Cambridge, MA 02142, USA

[2]Department of Chemical Engineering, Massachusetts Institute of Technology, Cambridge, MA 02139, USA

[3]Harvard-MIT divison of Health Sciences & Technology, Cambridge, MA 02139, USA

[4]Department of Biological Engineering, Massachusetts Institute of Technology, Cambridge, MA 02139, USA

[5]Department of Biological Engineering, University of Toledo, Toledo, OH 43606, USA

Abstract

The assembly, stability and timely disassembly of short interfering RNA (siRNA) nanocomplexes all have the potential to affect the efficiency of siRNA delivery and gene silencing. As such, the design of new probes that can measure these properties without significantly perturbing the nanocomplexes or their environment may facilitate the study and further development of new siRNA nanocomplexes. Herein, we study Förster resonance energy transfer (FRET)-labeled siRNA probes that can track the assembly, stability and disassembly of siRNA nanocomplexes in different environments. The probe is composed of two identical siRNAs, each labeled with a fluorophore. Upon nanocomplex formation, the siRNA-bound fluorophores become locally aggregated within the nanocomplex and undergo FRET. A key advantage of this technique is that the delivery vehicle (DV) need not be labeled, thus enabling the characterization of a large variety of nanocarriers, some of which maybe difficult or even impossible to label. We demonstrate proof-of-concept by measuring the assembly of various DVs with siRNAs and show good agreement with gel electrophoresis experiments. As a consequence of not having to label the DV, we are able to determine nanocomplex biophysical parameters such as the extracellular apparent dissociation constants (K_D) and intracellular disassembly half-life for several in-house and proprietary commercial DV's. Furthermore, the lack of DV modification allows for a true direct comparison between DVs as well as correlation between their biophysical properties and gene silencing.

Keywords

siRNA; FRET; Nanocomplex; Fluorescent Probe; polycation; lipid; lipidoid

Following the discovery of RNAi by Fire and Mello,[1] siRNAs have emerged as powerful tools for the regulation and silencing of endogenous genes. Recently, clinical studies have demonstrated evidence of RNAi in humans *via* systemic siRNA delivery.[2,3] These and other studies demonstrate the great potential of RNAi for the treatment of human diseases *via* the use of siRNA therapeutics. In general, to achieve delivery (both *in vitro* and *in vivo*), siRNAs must be conjugated or encapsulated with delivery vehicles (polymers, lipids and lipidoids among a few).[4-7] Following cellular delivery of the siRNA nanocomplex, disassembly must occur in order to facilitate loading of siRNA into the RNAi machinery.[8,9] Thus, formation and disassembly of siRNA nanocomplexes are critical to achieving efficient siRNA delivery and gene silencing.

In this article, our primary goal was to develop a simple, non-invasive probe that can track formation, stability and disassembly of any DV-siRNA nanocomplex in both extracellular and intracellular environments. To do this, two chemically identical siRNA molecules were labeled each at the 5′ end of the sense strand, one with AlexaFlour594 (siAF594, FRET donor) and the other with AlexaFlour647 (si647, FRET acceptor). AlexaFluor dyes were chosen because of their superior photostability, pH independence and extremely high FRET efficiency.[10] In the absence of a delivery vehicle, we expect the highly charged siRNAs to remain far from one another in solution due to electrostatic repulsion. Under these conditions, excitation of the donor should not result in FRET. However, in the presence of cationic delivery vehicles that cause local siRNA aggregation *via* charge neutralization, excitation of the donor should lead to energy transfer from the donor to the acceptor if the labeled-siRNAs in the nanocomplex are within the Förster radius of the FRET pair (8.5 nm, Scheme 1).

RESULTS AND DISCUSSION

To demonstrate proof-of-concept, we studied nanocomplex formation between our siRNA probes and two commercially available transfection agents; branched-polyethylene imine (b-PEI) and lipofectamine RNAiMax. The emission spectra for b-PEI/siRNA nanocomplexes are shown in Figure 1a. The b-PEI/siAF594-siAF647 pair was excited at 540 nm in order to minimize direct excitation of the acceptor. Also shown are the emission spectra of b-PEI/siAF594 and b-PEI/siAF647 alone (also excited at 540 nm). An increase in the b-PEI concentration leads to a reduction in the emission peak of the siAF594 donor (590-650 nm) and a subsequent increase in the emission peak of the siAF647 acceptor (650-720 nm). A FRET signal is reported (Figure 1b) as the ratio of the emission peak at 690 nm to that at 620 nm and gives an indication of the extent of nanocomplex formation. A similar phenomenon is observed with Lipofectamine-siRNA nanocomplexes (Figures 1c and 1d).

We validated the FRET emission curves by carrying out an electrophoretic mobility assay (EMA) and compare the results to quantified FRET data. As shown in Figure 1b, complete assembly is observed at a charge ratio (Nitrogen on b-PEI/Phosphate on siRNA, N/P) of 5/1 *via* both FRET and EMA. Treatment of b-PEI/siRNA nanocomplexes with heparin sulfate (an anionic destabilizing agent) resulted in the loss of FRET, which is an indication of siRNA release as confirmed by EMA. Similar results were also observed for the Lipofectamine-siRNA nanocomplexes (Figure 1d). All together, these set of experiments demonstrate the utility of the FRET-labeled siRNA probes for tracking the formation and disassembly of siRNA nanocomplexes.

Upon further inspection of Figure 1c, we observed that the FRET signal from the Lipofectamine-siRNA nanocomplexes decreases beyond a lipofectamine volume to siRNA weight ratio (μL/μg) of 20. In the case of b-PEI-siRNA nanocomplexes (Figure 1b), the decrease occurs above a charge ratio (N/P) of 5, albeit to a lesser extent. This bell-shaped

phenomenon was reproduced with a wide variety of DVs (Figure 2a). We attribute this decline to redissolution of the nanocomplexes as predicted by the two-state binding model for ligand-induced polyelectrolyte condensation.[11-15] According to this model (Figure S1),[13] siRNAs in the presence of DVs may either be in a starting or condensed phase. At high enough DV concentrations, thermodynamic equilibrium is shifted to favour the condensed phase (*i.e.* siRNA nanocomplexes). Yet, at even higher DV concentrations, these nanocomplexes may re-dissolve or swell leading to a decrease in FRET signal, as long as the siRNAs have available binding sites. The traditional FRET technique for monitoring nanocomplex formation, which involves labeled DV and siRNA, should be unable to capture the aggregation-redissolution phenomenon because re-dissolution or swelling as a result of excess positive charge only decreases condensation and not complexation. The latter actually increases. To test this theory, we labeled b-PEI with AlexaFluor 647 carried out a FRET assay with siAF594 as the donor. The results in Figure 2b show that the FRET signal increases until saturation is achieved at an N/P of 30, thus giving further validity to the assertions of the two-state model. The results in Figure 2b highlight a major difference between the interactions being measured by both FRET techniques. The FRET signal obtained from labeling both DV and siRNA gives us information regarding the binding interaction between the DV and siRNA, while our technique of labeling two identical siRNAs with a FRET pair gives us information regarding nanocomplex formation. It is important to be aware of this distinction so that the correct deductions can be made from acquired data when either of these techniques is exploited.

The FRET readout observed from these nanocomplexes is an indirect measure of DV induced siRNA aggregation, represented by $(S_1 - S_2)_{DV}$ in Equation (1), where S_1 and S_2 represent AlexaFluor 594 and 647 labeled siRNAs respectively. The relationship between $[(S_1 - S_2)_{DV}]$ and K_D, and that between $[(S_1 - S_2)_{DV}]$ and the FRET signal is given by Equation (2) and (3) (see supporting information for derivations).

$$S_1 + S_2 + DV \rightleftharpoons \left[(S_1 - S_2)_{DV} \right] + DV \tag{1}$$

$$\left[(S_1 - S_2)_{DV} \right] = \left[K_D + S_{1,tot} + S_{2,tot} - \sqrt{(K_D + S_{1,tot} + S_{2,tot})^2 - 4 S_{1,tot} S_{2,tot}} \right] / 2 \tag{2}$$

$$[FRET\ ratio - MIN] / [MAX - MIN] = \left[(S_1 - S_2)_{DV} \right] / S_{1,tot} \tag{3}$$

Two key assumptions are that $S_1 \simeq S_2$ (this was the case in all FRET experiments) and $\Delta[DV]$ is minimal. Equations (2) and (3) were fit to the FRET data by performing a non-linear regression analysis using K_D, MAX (Maximum FRET signal) and MIN (Minimum FRET signal) as fit parameters. This approach for determining K_D by method of dilution was adapted from You *et al.*[16] Examples of the equilibrium binding data for b-PEI, Dharmafect and Hiperfect along with their corresponding fits are given in Figure 3a (see Figure S2 in the supporting text for data on the other DVs). The K_D values obtained from the fitted equilibrium binding curves in Figure 3a were plotted as a function of DV/siRNA ratio (Figure 3b). As expected, we found that an increase in DV/siRNA ratio gives rise to a lower K_D, *i.e.* tighter associations between siRNAs. The simple model put forward in Equation (1) does not include a relationship for the re-entrant behavior of the complexes at extremely high DV concentrations and as such, Figure 3b does not reflect the re-entrant behaviour of the complexes at the high DV concentrations shown in Figure 2. Nevertheless, the apparent K_D values correctly model the behaviour of the siRNA nanocomplexes at lower DV/siRNA ratios.

Next, we focused on the use of the dual labeled-siRNA probe as a tool for evaluating the intracellular disassembly of nanocomplexes in live cells. This was done by transfecting HeLa cells with nanocomplexes containing the dual labeled-siRNA probes followed by analysis *via* confocal microscopy and flow cytometry. Proof of intact siRNA delivery complexes was provided by confocal microscopy as shown in the representative example of ND98 nanocomplexes transfected into HeLa cells in Figure 4a. Extensive co-localization of the two fluorophores is observed after incubating the cells for one hour. All ND98-siRNA nanocomplexes appear to be located in vesicular structures. The punctate structures showed strong co-localization (yellow) between the two fluorophores. Some single color vesicles (red or green only) were also observed, indicating that disassembled siRNA mostly tends to remain in similar endocytic vesicles, although small amounts amount may be routed to different vesicles. . To determine whether the observed vesicular co-localization of the two dyes is due to intact nanocomplexes, the transfected cells were also analyzed for FRET *via* flow cytometry. FRET was observed by exciting the cells at 561 nm with a yellow-green laser and monitoring the fluorescence emission through a 695/40 nm filter. The latter was normalized to the emission observed through the AlexaFluor594 channel. As shown by the representative examples in Figure 4b, a positive FRET signal was only observed for nanocomplexes containing the dual labeled-siRNA (dark green, light green and orange curves). These results confirm the ability of this dual labeled-siRNA probe to detect intact intracellular siRNA nanocomplexes. The cellular uptake experiments from Figure 4b were repeated at different time points and the results were quantified by fitting the data to a single-phase exponential decay curve (Figure 4c). The results in Figure 4d indicate that with the exception of Dharmafect which has a long intracellular disassembly half-life of almost 4 hours, most delivery vehicles (at a DV/siRNA ratio of 10) have a disassembly half-life that falls in the range of 30 minutes to 2 hours. Numerous factors such as chemical stability of the delivery vehicle and competing intracellular protein and nucleic acid interactions contribute to the rate and extent of intracellular disassembly of the siRNA nanocomplexes.

Finally, we examined how our measured K_D would correlate with the ability of the DVs to deliver siRNA and thus silence a luciferase reporter gene in a HeLa cell line. The results of the gene-silencing assay are shown in Figure 5a. In general, we observe that siRNA delivery and thus gene-silencing increases across all classes of DVs with increasing DV/siRNA ratio. However, the correlation between gene silencing and K_D reveals some interesting trends. First, under our experimental conditions, we observe that the following DVs; b-PEI, siPORT-Amine, ribojuice and siPORT-NEOFX, are unable to silence the reporter gene and thus show no correlation with their K_D's. Since these materials do show uptake and comparable intracellular half-lives, their lack of activity could be due to trafficking into inactive intracellular compartments. Among some of the DVs that do show RNAi activity, such as Hiperfect (blue) and C16-96 (green), we observe an inverse correlation between extent of gene silencing and K_D (Figure 5b). This suggests that nanocomplex dissociation plays an important role, and might even be a limiting factor in the activity of these nanocomplexes.

The discovery and use of siRNAs, both as a biological tool and therapeutic, has lead to the development of several tools and assays for detecting and quantifying the amounts of extracellular and intracellular siRNA. One of the most widely used approach for measuring assembly of siRNA delivery complexes is the dye exclusion assay.[17,18] This method relies upon the use of intercalating dyes, such as ethidium bromide, SYBR based dyes and Ribogreen, which fluoresce upon binding to "free" nucleic acids in solution. After siRNA complex formation, the siRNA molecules within the complex become inaccessible to the intercalating dyes; hence the exclusion assay. Although widely used in the siRNA delivery field, assays based on this detection strategy are indirect at best and provide very little biophysical information about the siRNA delivery complex. In addition, intercalating dyes

cannot be used for intracellular studies due to their non-specific mode of action. Our strategy, *via* the design of a pair of FRET-labeled siRNA probes, utilizes a distance-dependent FRET-based approach for monitoring the assembly and disassembly of siRNA nanocomplexes.

In context of siRNA delivery, FRET has been used primarily in two research directions. The first involves the use of FRET to monitor the intracellular integrity of siRNAs[19-21] *via* labeling one siRNA with two fluorophores (a FRET pair). The second direction involves the use of FRET to study the stability and intracellular trafficking of siRNA delivery complexes.[9,22] Experiments involving the latter employ fluorophore labeled siRNAs and delivery vehicles to monitor the assembly and disassembly of siRNA delivery complexes. Contrary to this technique, our FRET-labeled siRNA probe is unique because it allows us to gather similar information by labeling just the siRNA. As a result, two important advantages emerge. First, FRET is only reported when siRNA aggregation occurs and not for monomeric electrostatic binding events between the delivery vehicle and siRNA. Second, this technique does not require fluorescent labeling of the delivery vehicle. The latter is crucial when a large number of different polymers or lipids are being analyzed, some of which may be prove difficult to label or for which labeling causes a significant alteration of chemical function.

We validated our FRET-labeled siRNA probes by showing agreement with gel electrophoresis data and demonstrate universality by using this FRET technique with a wide range of siRNA delivery vehicles. We also distinguish key differences between our design and previous FRET-based methods used for detecting the assembly of siRNA delivery complexes within the framework of the two-state binding model. The results in Figure 2 capture the aggregation-redissolution phenomena as evidenced by the initial increase and subsequent decrease in FRET values. Redissolution of the nanocomplexes at high DV/ siRNA ratio's can be explained by saturation of binding sites (negatively charged phosphate groups) on siRNA by the DV, thus causing swelling or rupture of the nanocomplexes. An attempt to capture swelling or rupture by sizing measurements *via* light scattering was futile as the nanocomplexes formed with the DV's in Table 1 are polydisperse to begin with.

The data obtained from our FRET-labeled siRNA probes was used to determine parameters such as extracellular apparent binding constants (K_D) and intracellular disassembly half-lives ($t_{1/2}$) of the nanocomplexes. Both parameters report on the stability of the nanocomplexes and are important biophysical properties of the nanocomplexes that may find use in understanding structure-activity correlations where extent of gene silencing is currently the only activity readout. Using our limited data set of DV's in Table 1, an attempt was made to correlate the extent of gene silencing to the measured apparent dissociation constant. Among the delivery vehicles that were able to silence the expression of the Firefly luciferase reporter gene, reagents such as Hiperfect (blue) and C16-96 (green) showed an increasing ability to silence the reporter gene with decreasing K_D. The activity of these nanocomoplexes, in the selected range of DV/siRNA, might be limited by their stability so that tighter association with the DV (lower K_D) might increase their intracellular availability and access to the RNAi machinery. Other DV's such as Dharmafect (brown) show an initial increase in gene silencing with decreasing K_D, followed by a plateau. ND98 (yellow) appears insensitive to K_D while C14-113 (white) appears very sensitive to slight differences in K_D. It is important to note that each DV can employ diverse cellular pathways to gain cellular and cytoplasmic entry, which may also be dependent on multiple parameters such as other physicochemical properties of individual DV and the cell type being used. The latter might explain the diversity in correlations displayed in Figure 5b. Nonetheless, this study provides a versatile tool that enhances our ability to track and measure these properties in a

non-invasive manner and furthers the goal of understanding the different routes and mechanisms behind the nonviral delivery of siRNAs.

CONCLUSION

In summary, we have designed FRET-labeled siRNA probes for tracking the assembly and stability of siRNA nanocomplexes. Our technique holds a unique advantage over previous FRET-based techniques for measuring nanoparticle complex formation and dissociation because it obviates the need for labeling the DV. The latter allowed us to directly compare the assembly and stability of numerous in-house and commercially available siRNA nanocomplexes. Furthermore, using our FRET-labeled siRNA probes, we replicated the effect of reentrant aggregation (complex formation) and redissolution with increasing delivery vehicle concentration; a key feature of the two-state ligand-binding model for nucleic acid complex formation.[14,23] Furthermore, the FRET-labeled siRNA probes were used to quantify the extracellular stability of the siRNA delivery complexes *via* K_D measurements. The apparent K_D, a measure of DV-mediated siRNA affinity, was obtained from FRET data *via* an equilibrium-binding model. Due to the selective and non-destructive nature of this technique, we were also able to measure intracellular $t_{1/2}$ of the nanocomplexes in HeLa cells *via* flow cytometry. Finally, we obtained DV-specific correlations between K_D and extent of gene silencing in a HeLa cell line. Overall, the design of new probes that can provide information about the biophysical properties of siRNA delivery complexes in a non-destructive manner are key to informing the future design and discovery of efficient siRNA delivery vehicles that can eventually be translated to the clinical setting.

MATERIALS AND METHODS

Materials

siRNA duplexes labeled at the 5′ end of the sense strand with either Alexa Fluor594 or Alexa Fluor647 dyes were purchased from Integrated DNA Technologies (HPLC purified and desalted). The sequences were: (sense) 5′Alex594-GAUUAUGUCC GGUUAUGUAUU, 5′Alex647-GAUUAUGUCCGGUUAUGUAUU and (antisense) 5′-UACAUAACCGGACAUAAUCUU. Lipidoids were synthesized according to previous reports.[24,25] Ribojuice was purchased from Novagen. siPORT-NEOFX and siPORT-Amine were purchased from Ambion. Dharmafect 1 was purchased from Thermoscientific Dharmacon. Hiperfect was purchased from Qiagen. Branched polyethyleneimine (b-PEI, 25 kDa) and dimethylsulfoxide (DMSO) were purchased from Sigma-Aldrich. OptiMEM, phenol red-free DMEM, fetal bovine serum (FBS), 0.25% trypsin-EDTA, Alexa Fluor 647-NHS ester, Lipofectamine RNAiMAX and E-Gel 0.8% Agarose gels were obtained from Invitrogen. siRNA against firefly luciferase, siGL3 duplex (D001400-01-20), was purchased from Thermoscientific Dharmacon. Zeba Spin Desalting Columns (7K MWCO) were obtained from Thermoscientific PIERCE. 4 mL Amicon Ultra-4 Centrifugal filters were obtained from Millipore.

Synthesis of b-PEI-Alexa Fluor647

b-PEI was dissolved in borate buffer and the pH was adjusted to 8.0 using 1.0 N HCl. Alexa Fluor647-NHS ester was dissolved in DMSO at a concentration of 20 mg/mL. The Alexa Fluor647-NHS ester/DMSO solution (50 μL) was then added to 385 μL of the b-PEI solution in borate buffer. The mixture was vortexed and incubated in the dark for 2 hours. The entire mixture was then dialyzed four times with acetate buffer using an Amicon Ultra-4 centrifugal filter. After the last centrifugal spin, the sample was diluted to 1 mL and passed

through a Zeba Spin Desalting Column, prewashed with acetate buffer. b-PEI concentration in the b-PEI-Alexa Fluor647 conjugate was determined using the following equation:

$$[b - \text{PEI}] = [\text{A}(280) - \text{A}(650) * \text{CF}] / \varepsilon_{(b-\text{PEI})}$$

where A(280) and A(650) are the absorbance at 280 and 650 nm, CF is the correction factor (0.03) accounting for the absorbance of the Alexa Fluor647 dye at 280 nm and $\varepsilon_{(b\text{-PEI})}$ is the extinction coefficient of b-PEI.

Cell culture

HeLa cells, stably expressing firefly luciferase and *Renilla* luciferase, were generously donated by Alnylam pharamceuticals. The cells were maintained in phenol red-free DMEM media (no antibiotics) with 10% FBS (growth media) at 37°C in a 5% CO_2 humidified atmosphere.

FRET assays

siRNA labeled with Alexa Fluor594 and Alexa Fluor647, referred to as siAF594 and siAF647 respectively, were used as 50:50 mixtures in all FRET experiments. Delivery vehicles were typically added to the siRNA solution in acetate buffer in a black 96-well assay plate at the desired wt/wt (lipidoids/siRNA), N/P (b-PEI, +/-) or µL/wt (other commercial delivery vehicles/siRNA) ratio's. The resulting solution was then diluted with OptiMEM, DMEM or acetate buffer to 100 µL to achieve a 100 nM siRNA concentration unless stated otherwise. After incubation for 10 minutes, the samples were excited at 540 nm and the fluorescence intensity was read at 690 and 620 nm using a Tecan Safire 2 Microplate reader. FRET was determined as the ratio of the fluorescence intensities at 690/620 nm. The FRET signals for all samples were normalized to a control FRET signal from the siAF594 and siAF647 pair without any delivery vehicle. All experiments were conducted at room temperature unless stated otherwise. For K_D measurements, siRNA delivery complexes were prepared at 0.8 – 1.6 µM siRNA concentrations and serially diluted over three orders of magnitude in OptiMEM (lipids and polymers) or DMEM (lipidoids). FRET was measured as described above at room temperature using a Tecan Safire 2 Microplate reader. Absorbance, excitation and emission scans were also recorded in 96-well plates with the Tecan Safire 2 Microplate reader. Optically clear plates were used for absorbance scans while black assay plates were used for excitation and emission scans.

Agarose Gel electrophoresis of siRNA delivery complexes

Delivery vehicles were complexed with siGL3 at different wt/wt, N/P, and µL/wt ratio's in OptiMEM. 10 µL of the siRNA delivery complex containing 0.1 µg siGL3 was mixed with 40% glycerol (2 µL) and loaded on an E-Gel 0.8% agarose gel prestained with ethidium bromide and run for 15 minutes. For experiments with heparin sulfate or SDS, 10 µL of the siRNA delivery complex containing 0.1 µg siGL3 was mixed with 1.1 µL heparin sulfate (2 mg/mL) or 1.0 µL SDS (100 mg/mL). This mixture was then added to 40% glycerol (2 µL), loaded on an E-Gel 0.8% agarose gel prestained with ethidium bromide and run for 15 minutes. At the end of the run, the gel was removed and imaged on a BioRad Gel Doc XR gel imaging system.

Evaluation of intracellular disassembly half-life via flow cytommetry

For experiments with lipidoids and b-PEI, HeLa cells were seeded in a 12-well plate at a density of 1.5×10^5 cells/well and maintained for 24 hours. Lipidoid-siRNA complexes were prepared at a 10/1 (wt/wt) ratio in acetate buffer (pH 5.0) and diluted with growth

media to give a final siRNA concentration of 100 nM. b-PEI-siRNA complexes were prepared at a 5/1 (N/P) ratio in OptiMEM and diluted with growth media to give a final siRNA concentration of 100 nM. The media on the cells was aspirated and replaced with 1 mL of the lipidoid-siRNA complexes or b-PEI-siRNA complexes in growth media. The cells were transfected for the indicated amount of time. All experiments were carried out in triplicates. For experiments with other commercial delivery vehicles, HeLa cells were seeded in a 12-well plate at a density of 1.5×10^5 cells/well and maintained for 24 hours. On the day of transfection, the media on the cells was aspirated and replaced with 0.73 mL of fresh growth media. siRNA delivery complexes were prepared at a 10/1 (μL/wt) ratio in 70 μL OptiMEM and added to the cells to give a 50 nM final siRNA concentration. The cells were transfected for the indicated amount of time. For flow cytometry analysis, the transfection media was aspirated and the cells were washed with calcium and magnesium free PBS, trypsinized with 0.25 mL 0.25% trypsin-EDTA, neutralized with 0.75 mL growth media and collected in 0.5 mL eppendorf tubes. The cells were pelleted ($500 \times g$ for 5 mins) to remove the trypsin solution *via* aspiration, washed with a 10% growth media in PBS solution and resuspended in 0.5 mL of 10% growth media in PBS. The cells were sieved with a cell strainer (BD Bioscience) prior to flow cytommetry analysis. 10,000 events were monitored and evaluated by a BD LSR II HTS flow cytometer (BD Bioscience). A 561 nm (yellow-green) excitation laser was used excite the Alexa Fluor594 fluorophore and its emission was observed with a 610/20 nm filter. A 633 nm (red, HeNe) laser was used to excite the Alexa Fluor647 fluorophore and its emission was observed with a 660/20 nm filter. Each channel was compensated for bleed through using single fluorophore controls. FRET was monitored by exciting the samples with a 561 nm excitation laser and observing their emission with a 695/40 nm emission filter set. The emission signal obtained was normalized to the emission signal obtained from the Alexa Fluor594 channel to correct for the total siRNA delivery complex uptake at each time point.

In vitro siRNA transfection assay

HeLa cells (15,000 cells/well) were seeded into the wells of an opaque white 96-well plate (Corning-Costar) and allowed attach overnight in growth media (phenol red-free DMEM with 10% FBS). Cells were transfected with 50 ng of siGL3 complexed with the delivery vehicles in Table 1 at different wt/wt, μL/wt or N/P ratio's in quadruplicates. Lipidoids were complexed with siGL3 in acetate buffer (pH 5.0) prior to transfection. All other delivery vehicles were complexed with siGL3 in OptiMEM prior to transfection. The siRNA delivery complexes were allowed to sit for at least 5-10 minutes to allow for complex formation after which they were transferred to the plated cells in complete growth media. HeLa cells were transfected for 24 hours. The Firefly and *Renilla* luciferase expression was analyzed using Dual-Glo assay kits (Promega). Luminescence was measured using a Tecan Safire 2 Microplate reader.

Confocal Microscopy

50,000 Hela cells per well were plated in chambered glass coverslips overnight. Cells were then exposed to formulated ND98 particles[26] containing the siRNA FRET pair (a 50:50 mixture of siAF594 and siAF647) for 1 hour, followed by incubation with Hoechst (2 μg/ml) for nuclear stain. The cells were washed with PBS and imaged using a Perkin Elmer Spinning Disk Confocal Microscope. 3D z-stacks were captured and processed utilizing the Ultra View ERS software. Images are shown as a top view 3D image.

Supplementary Material

Refer to Web version on PubMed Central for supplementary material.

Acknowledgments

REFERENCES

1. Fire A, Xu S, Montgomery MK, Kostas SA, Driver SE, Mello CC. Potent and Specific Genetic Interference by Double-Stranded RNA in Caenorhabditis Elegans. Nature. 1998; 391:806–811. [PubMed: 9486653]

2. Davis ME, Zuckerman JE, Choi CHJ, Seligson D, Tolcher A, Alabi CA, Yen Y, Heidel JD, Ribas A. Evidence of RNAi in Humans From Systemically Administered siRNA *via* Targeted Nanoparticles. Nature. 2010; 464:1067–1070. [PubMed: 20305636]

3. Pharmaceuticals A. Alnylam Demonstrates RNAi in Man with Systemically Delivered RNAi Therapeutics - News Release. 2011

4. Wagner E. Polymers for siRNA Delivery: Inspired by Viruses to Be Targeted, Dynamic, and Precise. Acc. Chem. Res. 2011

5. Whitehead KA, Langer R, Anderson DG. Knocking Down Barriers: Advances in siRNA Delivery. Nat Rev Drug Discov. 2009; 8:129–138. [PubMed: 19180106]

6. Jeong JH, Mok H, Oh Y-K, Park TG. siRNA Conjugate Delivery Systems. Bioconjugate Chem. 2009; 20:5–14.

7. Schroeder A, Levins CG, Cortez C, Langer R, Anderson DG. Lipid-Based Nanotherapeutics for siRNA Delivery. J. Intern. Med. 267:9–21. [PubMed: 20059641]

8. Waite CL, Sparks SM, Uhrich KE, Roth CM. Acetylation of PAMAM Dendrimers for Cellular Delivery of siRNA. BMC Biotechnol. 9:38–38. [PubMed: 19389227]

9. Lee H, Kim I-K, Park TG. Intracellular Trafficking and Unpacking of siRNA/Quantum Dot- PEI Complexes Modified with and Without Cell Penetrating Peptide: Confocal and Flow Cytometric FRET Analysis. Bioconjugate Chem. 2010; 21:289–295.

10. Johnson, IJ.; Spence, M., editors. The Molecular Probes Handbook, a Guide to Fluorescent Probes and Labeling Technologies. 11th ed..

11. Pelta J, Livolant F, Sikorav JL. DNA Aggregation Induced by Polyamines and Cobalthexamine. J. Biol. Chem. 1996; 271:5656–5662. [PubMed: 8621429]

12. Saminathan M, Antony T, Shirahata A, Sigal LH, Thomas T, Thomas TJ. Ionic and Structural Specificity Effects of Natural and Synthetic Polyamines on the Aggregation and Resolubilization of Single-, Double-, and Triple-Stranded DNA†. Biochemistry. 1999; 38:3821–3830. [PubMed: 10090772]

13. Teif VB. Ligand-Induced DNA Condensation: Choosing the Model. Biophys. J. 2005; 89:2574–2587. [PubMed: 16085765]

14. Lando DY, Teif VB. Modeling of DNA Condensation and Decondensation Caused by Ligand Binding. J. Biomol. Struct. Dyn. 2002; 20:215–222. [PubMed: 12354073]

15. Porschke D. Nature of Protamine-DNA Complexes: a Special Type of Ligand Binding Co-Operativity. J. Mol. Biol. 1991; 222:423–433. [PubMed: 1960734]

16. You X, Nguyen AW, Jabaiah A, Sheff MA, Thorn KS, Daugherty PS. Intracellular Protein Interaction Mapping with FRET Hybrids. Proc. Natl. Acad. Sci. USA. 2006; 103:18458–18463. [PubMed: 17130455]

17. Eastman SJ, Siegel C, Tousignant J, Smith AE, Cheng SH, Scheule RK. Biophysical Characterization of Cationic Lipid:DNA Complexes. BBA-Biomembranes. 1997; 1325:41–62. [PubMed: 9106482]

18. Ferrari ME, Nguyen CM, Zelphati O, Tsai Y, Felgner PL. Analytical Methods for the Characterization of Cationic Lipid-Nucleic Acid Complexes. Hum. Gene Ther. 1998; 9:341–351. [PubMed: 9508052]

19. Raemdonck K, Remaut K, Lucas B, Sanders NN, Demeester J, De Smedt SC. *In Situ* Analysis of Single-Stranded and Duplex siRNA Integrity in Living Cells. Biochemistry. 2006; 45:10614–10623. [PubMed: 16939213]

20. Jarve A, Muller J, Kim IH, Rohr K, MacLean C, Fricker G, Massing U, Eberle F, Dalpke A, Fischer R, et al. Surveillance of siRNA Integrity by FRET Imaging. Nucl. Acids Res. 2007; 35:e124. [PubMed: 17890733]

21. Uhler SA, Cai D, Man Y, Figge C, Walter NG. RNA Degradation in Cell Extracts: Real- Time Monitoring by Fluorescence Resonance Energy Transfer. J. Am. Chem. Soc. 2003; 125:14230–14231. [PubMed: 14624543]

22. Jiang S, Zhang Y. Upconversion Nanoparticle-Based FRET System for Study of siRNA in Live Cells. Langmuir. 2010; 26:6689–6694. [PubMed: 20073488]

23. Teif VB. Ligand-Induced DNA Condensation: Choosing the Model. Biophys. J. 2005; 89:2574–2587. [PubMed: 16085765]

24. Love KT, Mahon KP, Levins CG, Whitehead KA, Querbes W, Dorkin JR, Qin J, Cantley W, Qin LL, Racie T, et al. Lipid-Like Materials for Low-Dose, *in Vivo* Gene Silencing. Proc. Natl. Acad. Sci. USA. 2010; 107:1864–1869. [PubMed: 20080679]

25. Akinc A, Zumbuehl A, Goldberg M, Leshchiner ES, Busini V, Hossain N, Bacallado SA, Nguyen DN, Fuller J, Alvarez R, et al. A Combinatorial Library of Lipid-Like Materials for Delivery of RNAi Therapeutics. Nat. Biotech. 2008; 26:561–569.

26. Akinc A, Goldberg M, Qin J, Dorkin JR, Gamba-Vitalo C, Maier M, Jayaprakash KN, Jayaraman M, Rajeev KG, Manoharan M, et al. Development of Lipidoid-siRNA Formulations for Systemic Delivery to the Liver. Mol. Ther. 2009; 17:872–879. [PubMed: 19259063]
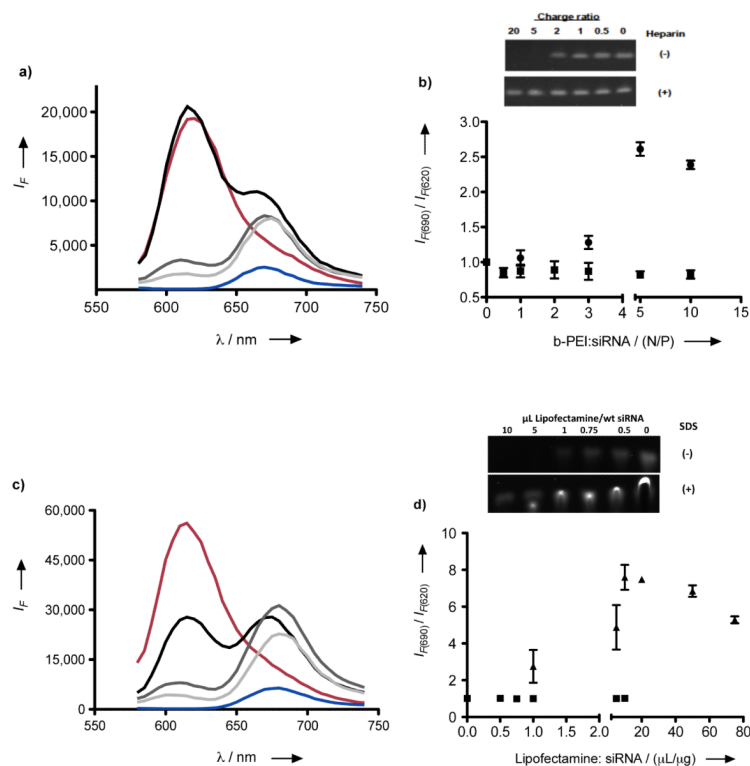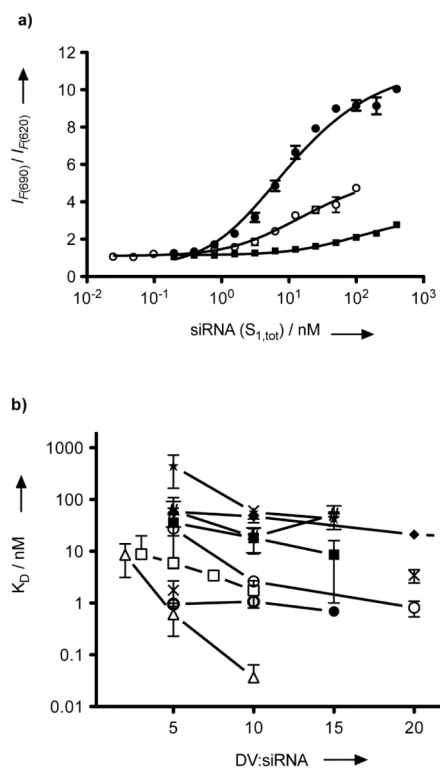
Figure 1.
a) Fluorescence emission scans (540 nm excitation) of b-PEI nanocomplexes with siAF594 (red), siAF647 (blue), and an equimolar mixture of siAF594-siAF647 (black to gray) at increasing amounts of b-PEI. N/P (Nitrogen to Phosphate) ratio's; 1:1-black, 5:1- gray and 10:1-light gray. b) Agarose gel electrophoresis and ratiometric FRET signal from b-PEI:siRNA nanocomplexes with (■) and without (•) heparin sulphate. c) Fluorescence emission scans (540 nm excitation) of Lipofectamine nanocomplexes with siAF594 (red), siAF647 (blue), and an equimolar mixture of siAF594-siAF647 at increasing amounts of Lipofectamine. µL/µg (volume of DV to weight of siRNA) ratio's; 2:1-black, 5:1- gray and 10:1-light gray. b) Agarose gel electrophoresis and ratiometric FRET signal from Lipofectamine:siRNA nanocomplexes with (■) and without (▲) SDS. The siRNA in gels were visualized after staining with ethidium bromide.
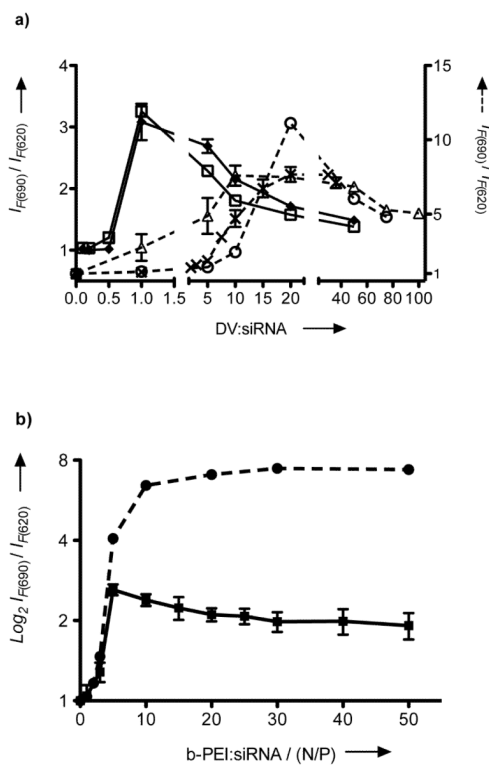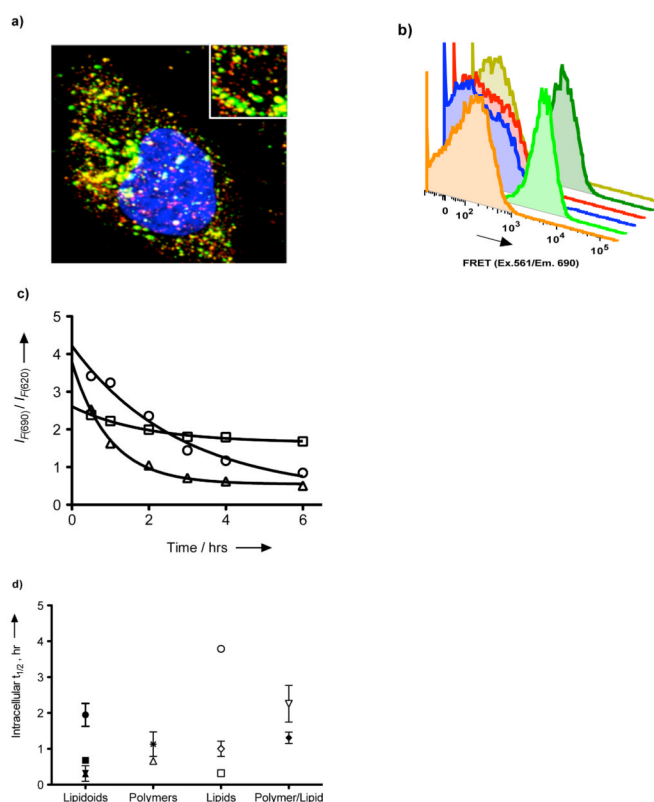
Figure 2.
a) Response of ratiometric FRET to increasing amounts of ($\blacklozenge$) siPORT-Amine, ($\square$) Ribojuice, (Δ) Lipofectamine, ($\times$) ND98, and ($\bigcirc$) Hiperfect. The total siRNA concentration was fixed at 100 nM. All DV/siRNA ratios are in µL/µg except for ND98, which is in µg/µg. b) Ratiometric FRET (Log scale) of b-PEI-AF647/siAF594 (•) and b-PEI/siAF594-siAF647 ($\blacksquare$) nanocomplexes. Lines are drawn between the data points to aid visualization.
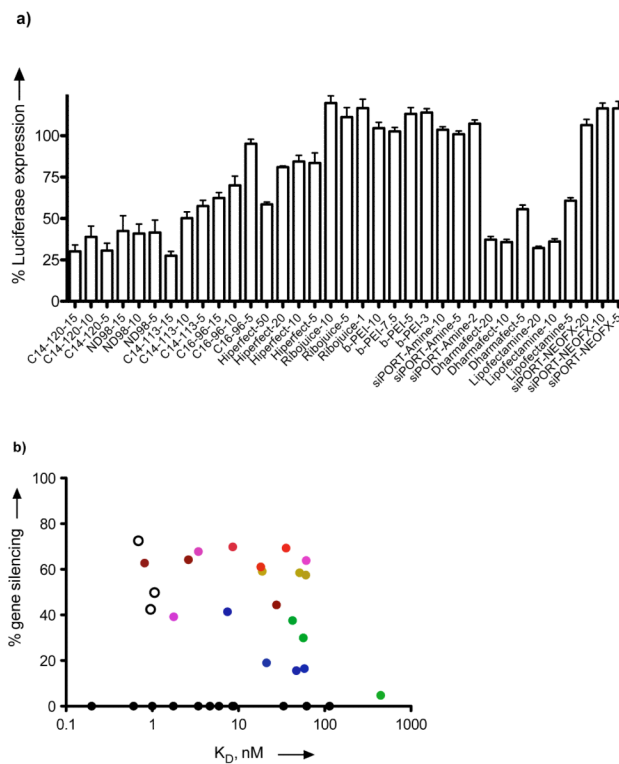
Figure 3.
a) Ratiometric FRET data of (•) Dharmafect, (○) b-PEI and (■) Hiperfect were obtained *via* serial dilution of the complexes in media. The lines are linear regression fits of Eq. (2) and (3). b) Inverse relationship between apparent K_D and DV/siRNA ratio of (△) siPORT-NEOFX, (•) C14-113, (□) b-PEI, (○) Dharmafect, (■) C14-120, (×) Lipofectamine, (◆) Hiperfect, (⋆) C16-96, and (⌗) ND98 nanocomplexes. Solid and broken lines are drawn between the data points to aid visualization.

Figure 4.
a) Confocal microscopy image of a HeLa cell transfected with nanocomplexes of ND98 with a 1:1 mixture of siAF594 and siAF647. The green dots represent siAF594 and the red dots represent siAF647. Co-localization of two fluorophores (red and green) appears as a yellow color. The nucleus is stained blue with Hoechst dye. The inset at the top right corner is a magnification of the endosomal vesicles. b) HeLa cells were transfected with the following nanocomplexes for one hour in growth media, washed, filtered and analyzed by flow cytommetry: Cells alone (dark yellow), ND98/siAF594 (red) and ND98/siAF647 (blue), ND98/siAF594-AF647 (dark green), C14-113/siAF594-AF647 (light green) and PEI/siAF594-AF647 (orange). The samples were excited with a 561 nm laser and their emission was observed at 690 nm. A positive FRET signal is observed only with nanocomplexes containing both siRNA-fluorophores. c) Normalized intracellular FRET of ND98 (○), C14-113 (△) and b-PEI (□) as a function of time (hours) as measured by flow cytometry. Each data point represents the average of three experiments. Data points for each siRNA delivery complex were fit to a single-phase exponential decay curve to determine intracellular half-life. d) Intracellular half-lives of the nanocomplexes grouped according to delivery vehicle type; (•) ND98, (■) C14-113, (▼) C16-96, (▲) C14-120 (·) siPORT-Amine, (△) PEI, (○) Dharmafect, (◇) siPORT-NEOFX, (□) RNAiMAX, (▽) Ribojuice, (◆) Hiperfect

Figure 5.
a) HeLa cells expressing both Firefly and *Renilla* luciferase were transfected using the delivery vechicles listed in Table 1 with 50 ng of siRNA against Firefly luciferase. The extent of gene silencing is reported as ratio of the Firefly to *Renilla* luciferase expression relative to that of untreated cells (100%). Nomenclature for the x-axis is as follows: delivery agent - μg reagent/μg siRNA (ND98, C14-113, C16-96, C14-120), delivery agent - μL reagent/μg siRNA (Ribojuice, Hiperfect, Dharmafect, siPORT-Amine and siPORT-NEOFX) and delivery agent - Nitrogen on reagent/Phosphate on siRNA (b-PEI). b) Colored dots show the relationship between the extent of gene silencing and apparent K_D of individual delivery vehicles. Hiperfect (blue), Dharmafect (brown), Lipofectamine (purple), C16-96 (green), ND98 (yellow), C14-113 (white) and C14-120 (red). Ribojuice, b-PEI, siPORT-Amine, and siPORT-NEOFX (black).
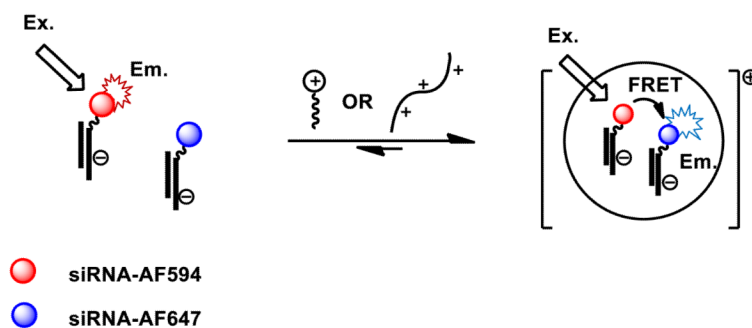
Scheme 1.
Excitation of the FRET-labeled siRNA probes at 540 nm in solution primarily results in the emission of siRNA-AF594 (siAF594) at 620 nm. Upon nanocomplex formation, excitation at 540 nm leads to FRET within the nanocomplex as characterized by the emission from siRNA-AF647 (siAF647) at 690 nm. FRET is quantified as the ratio of the fluorescence intensity at 690 nm to that at 620 nm.

TABLE 1

TYPE	DELIVERY VEHICLE (DV)
Cationic Lipid	Lipofectamine, siPORT-NEOFX, Dharmafect
Polyamine	siPORT-Amine, b-PEI (25 kDa)
Lipidoids [a]	ND98, C14-120, C14-113, C16-96
Polymer/lipid blend	Hiperfect, Ribojuice

[a] Previously published novel delivery materials[24,26]